PERGAMON

International Journal of Solids and Structures 40 (2003) 6767–6779

INTERNATIONAL JOURNAL OF SOLIDS and STRUCTURES

www.elsevier.com/locate/ijsolstr

Active and passive magnetic constrained damping treatment

Huiming Zheng [a,*], Ming Li [b], Zeng He [a]

[a] *Department of Mechanics, Huazhong University of Science and Technology, Wuhan, Hubei Province 430074, PR China*
[b] *Educational Department of Wuhan Iron and Steel Corporation, Wuhan, Hubei Province 430083, PR China*

Received 9 January 2003; received in revised form 11 August 2003

Abstract

This paper has presented a new class of active and passive magnetic constrained layer damping (APMCLD) treatment for controlling vibration of three-layer clamped–clamped beams. Firstly, optimal placement strategies of discrete patches are investigated. The predictions of model are validated experimentally using three-layer clamped–clamped beams treated with fully or segmented passive magnetic constrained layer damping (MCLD) treatments. The results indicate that full MCLD treatment induces less improvement of damping characteristics. Also, the obtained results illustrate that, the improvement of damping performance using two-patched MCLD treatment becomes more apparent at the first mode compared to the corresponding performance using a single-patched MCLD treatment when the total length of damping layer is from $0.3L$ to $0.65L$ under considered magnetic force. Further, damping performances of APMCLD using several control strategies including simple PD controllers are investigated. The analytical results show that it induces less improvement of damping characteristics for higher modes using simple positive proportional feedback controllers whereas higher modes can been suppressed effectively using negative derivative feedback controllers. For broad band control of structural vibration, it is more effective using APMCLD treatments with combined proportional and derivative controllers. Moreover, the MCLD treatment still plays an important role in damping out structural vibrations even though active control systems fail.

Keywords: Clamped–clamped beam; Electromagnetic actuator; Damping treatment; Vibration control; Loss factor

1. Introduction

Because of material, thermal, package, location or cost constraint, partially covered passive constrained layer damping treatments (PCLD) are often used to damp out a wide variety of vibration of flexible structures (Kung and Singh, 1998). The PCLD, however, lacks the ability to compensate for changes in operating or environmental conditions. In order to enhance damping characteristics, numerous papers reported active and passive piezoelectric ceramic layer damping hybrid treatments (APPCLD) (Reader and Sauter, 1993; Shields et al., 1998). Although APPCLD treatments have proved to be successfully in damping out structural vibration, ceramics are brittle and their toughness and fatigue strength are not

* Corresponding author. Tel.: +86-2787-544740; fax: +86-2787-543338.
E-mail address: hezeng41@sohu.com (Z. He).

0020-7683/$ - see front matter © 2003 Elsevier Ltd. All rights reserved.
doi:10.1016/j.ijsolstr.2003.08.011

Nomenclature

$D_{t1} = \frac{1}{12} E_1 b h_1^3$ bending rigidity of the primary beam
E_i Young's modulus of the ith layer
G storage shear modulus of the damping layer
β loss factor of damping layer
η loss factor of beam
$G_c = G(1 + i\beta)$ complex shear modulus of damping layer
m_1 mass per unit length of the primary beam
$D_t = b(E_1 h_1^3 + E_3 h_3^3)/12$ bending rigidity of the sandwich section
b width of beam
m mass density per unit length of sandwich section
m_{mag} mass of a magnet
h_{mag} thickness of a magnet
M_i bending moment of cross-section
S_i shear force of cross-section
L_0 total length of a single or two patches
L total length of beam
h_i thickness of the ith layer
ρ_i mass density of the ith layer material
$A_i = bh_i$ transverse cross area of the ith layer
u_i alternating axial displacement of ith layer
w transverse displacement of the beam
t time

sufficient against externally applied shock loading and cyclic stress. The concept of magnetic constrained layer damping treatment (MCLD) is introduced (Ruzzene et al., 2000; Baz and Poh, 2000). A finite element model was developed to study performance characteristics of a fully covered cantilever beam with MCLD treatment (Ruzzene et al., 2000) and the improvement of damping characteristics was validated experimentally (Baz and Poh, 2000). Although the MCLD does not require for its operation any electronic sensors or control circuitry, the ability to compensate for changes in operating or environmental conditions is still limited.

Generally, cantilever beams are very flexible structures and they become more flexible when beams are treated with MCLD (Ruzzene et al., 2000; Baz and Poh, 2000), it is unsuitable using MCLD treatment in some cases. Amount of clamped–clamped beamlike elements whose stiffness is higher than that of cantilever beamlike elements exist in structures ranging from machines to space vehicles. On some of them instruments are fixed and also the elements themselves need to eliminate destructive resonance. It is therefore the purpose of this study to investigate the improvement of damping characteristics for a clamped–clamped beam using segmented MCLD treatment and further introduce the new class of active and passive magnetic constrained layer damping treatment (APMCLD) as a viable alternative to active and passive surface treatments. As the APMCLD utilizes electromagnetic actuators, it achieves actuation performance that is much higher than that of the APPCLD. With such capabilities, the APMCLD can provide a viable means for controlling large amplitudes of vibration.

In the present paper, the emphasis is placed on comparing the damping performance of clamped–clamped beams treated with one or two MCLD patches for selecting optimal placement strategies of

discrete patches and on investigating theoretically the effectiveness in controlling multi-modes of vibrations using simple proportional or/and derivative controllers. Such investigations would help to determinate design guidelines of APMCLD treatments.

The paper is organized in six sections. In Section 1, a brief introduction is given. The concept of APMCLD is presented in Section 2. In Section 3, the analytical model is derived employing Hamilton's principle. The experimental performance of beam/MCLD and optimal placement strategies of discrete patches are investigated in Section 4. In Section 5, the damping performance of APMCLD using simple proportional and derivative controller is evaluated theoretically. In Section 6, the conclusions are given.

2. The concept of APMCLD treatment

The concept of APMCLD can be best understood by considering the schematic representation of clamped–clamped sandwich beams shown in Fig. 1. Fig. 1(a) and (b) shows two possible configurations of discrete patches of same total length L_0, where a single patch is placed near the left end of beam with a small offset as shown in Fig. 1(a) or two patches symmetrically covered from each of both fixed ends with a small offset as shown in Fig. 1(b). The constraining layers (CL) are fitted with root magnets whereas integrated electromagnetic coils are placed in the base instead of permanent magnets as described by Ruzzene et al. (2000) and Baz and Poh (2000). The integrated electromagnetic coil consists of a self-sense coil and electromagnetic coil with ferromagnetic material as described in the papers (Lin, 1998; Changhwan and Kyihwan, 1999). The self-sense coil picks up gap variation signal between electromagnetic coil and permanent magnet. The pickup signal would be amplified and fed back to activate the electro-magnetic actuator under several control strategies including simple PD controllers. When the beam treated only with MCLD is in undeflected configuration, static magnetic attractive force resulting from magnets and ferromagnetic material produces static shear strains γ_0 in the viscoelastic layer. Fig. 1(c) shows deflected beam treated only

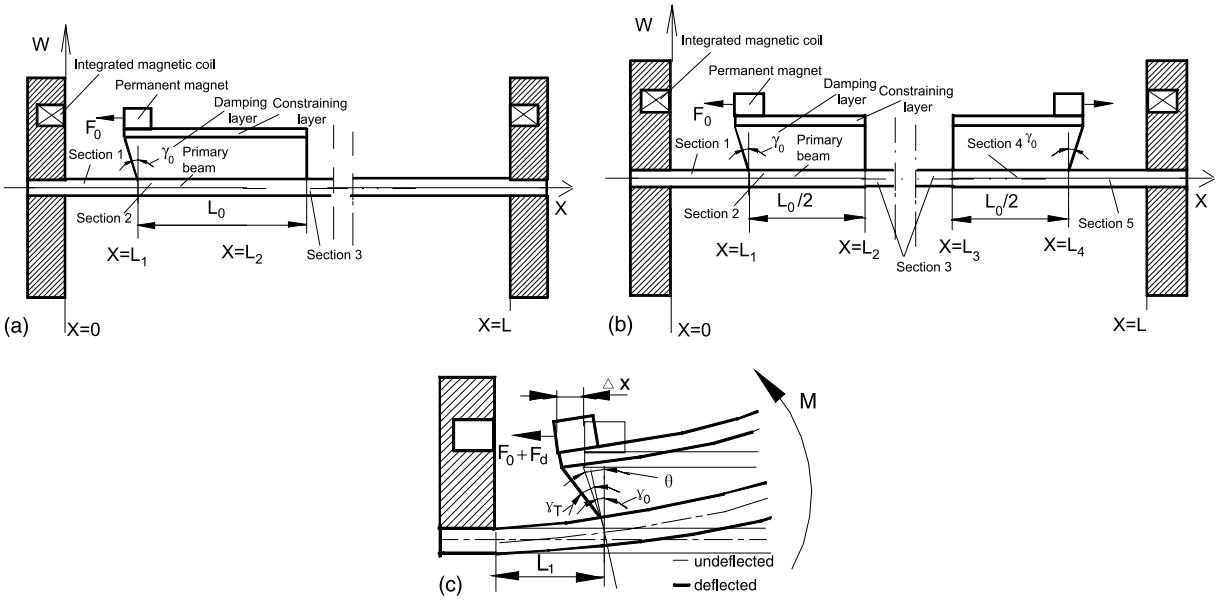

Fig. 1. Magnetic constraining damping treatment. (a) Undeflected beam treated with a sing APMCLD patch, (b) undeflected beam treated with two APMCLD patches and (c) deflected configuration.

with MCLD under the action of an external bending moment **M**. Due to the moment **M**, the gap between the magnets decreases, causing magnetic attraction force rise, the increment of shear strain $\gamma_{TM} = \gamma_T - \gamma_0$ is higher than the shear strain of the PCLD under external load of same moment **M**. Increasing the shear strain enhances the energy dissipation. When the beam is treated with APMCLD, it is possible to enhance the shear strain of VEM and significant improvement of damping characteristics may be realized.

3. Analytical modeling

The beam can be separated into several sections either without or with damping patches. The sections without patch are ordinary beams and the sections with patch are sandwich configurations.

Now let us consider the vibration of sandwich Section 2 shown in Fig. 1(a) and (b). The following assumptions are made in the analysis: (1) the beam deflection is small and uniform across any section; (2) the primary layer and the constraining layer are assumed to be isotropic; (3) the longitudinal and rotary inertia effects of the beam are neglected; (4) the damping layer carrying shear, but no direct stress, are assumed to be linear viscoelastic; and (5) no slip occurs at the interface between the layers.

We choose static equilibrium state as a reference position. The longitudinal displacements and shear angle as follows refer to the variation with respect to the reference position.

The potential energy of Section 2 is

$$\begin{aligned} V &= (V_1 + V_3)_{\text{bending}} + (V_1 + V_3)_{\text{extension}} + (V_c)_{\text{shearing}} \\ (V_1 + V_3)_{\text{bending}} &= \frac{1}{2}\int_{L_1}^{L_2} D_t \left(\frac{\partial^2 w}{\partial^2 x}\right)^2 \mathrm{d}x \\ (V_1 + V_3)_{\text{extension}} &= \frac{1}{2}\int_{L_1}^{L_2} E_1 A_1 \left(\frac{\partial u_1}{\partial x}\right)^2 \mathrm{d}x + \frac{1}{2}\int_{L_1}^{L_2} E_3 A_3 \left(\frac{\partial u_3}{\partial x}\right)^2 \mathrm{d}x \\ (V_c)_{\text{shearing}} &= \frac{1}{2}\int_{L_1}^{L_2} G_c A_c \gamma_c^2 \,\mathrm{d}x \end{aligned} \tag{1}$$

After neglecting longitudinal and rotary inertia and assuming the mass of permanent magnet concentrate at $x = L_1$. The total kinetic of Section 2 is

$$T = \frac{1}{2}\int_{L_1}^{L_2} \left[m\left(\frac{\partial w}{\partial t}\right)^2 \mathrm{d}x \right] + \frac{1}{2} m_{\text{mag}} \left(\frac{\partial w}{\partial t}\right)^2 \Big|_{x=L_1} \tag{2}$$

The fourth assumption implies that the sum of forces in the longitudinal direction is zero, i.e.

$$(EA)_1(\partial u_1/\partial x) + (EA)_3(\partial u_3/\partial x) = 0 \tag{3}$$

thus

$$u_1 = -c - [(EA)_3/(EA)_1]u_3 \tag{4}$$

the constant c is added so as to have an appropriate longitudinal displacement distribution. Note that this constant c has been ignored by many prior researchers but it is retained here since it plays an important role in deriving differential equations and boundary conditions.

In Fig. 2(a), we have the relationships:

$$\gamma_c = [H(\partial w/\partial x) + u_3 - u_1]/h_c = [H(\partial w/\partial x) + c + pu_3]/h_c \tag{5}$$

where $H = h_c + \frac{1}{2}(h_1 + h_3)$, $p = 1 + (EA)_3/(EA)_1$.

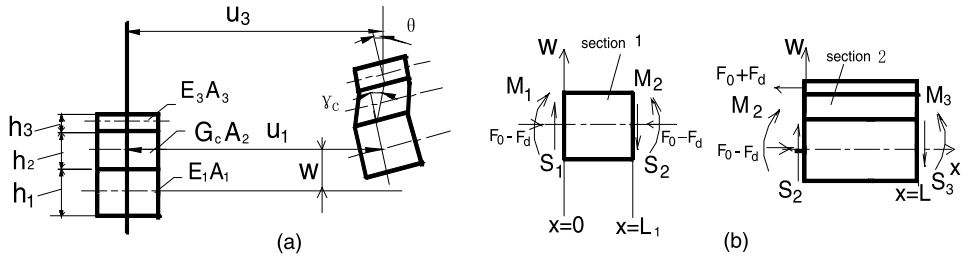

Fig. 2. The deformation and loads. (a) The geometry and deformation of Section 2, (b) Sections 1 and 2 with loads and moments.

Since the length of Section 1 is very short, the effect of pressure on work is negligible. Work done by external force is given by

$$W = \left[-M_2\left(\frac{\partial w_2}{\partial x}\right) + S_2 w_2 \right]\Big|_{x=L_1} + W_{\text{mag}}\Big|_{x=L_1} + \left[M_3\left(\frac{\partial w_2}{\partial x}\right) - S_3 w_2 \right]\Big|_{x=L_2} \tag{6}$$

where W_{mag} is work done by magnetic force F_{mag}. F_{mag} is x-direction component of the magnetic force. $F_{\text{mag}} = F_0 + F_{\text{d}}$, F_0 is the static component, F_{d} is the dynamic component. Since the sum of work done by the static component F_0 acting on the primary and constraining layer is zero, work done by F_{d} is only considered.

When APMCLD treatments operate in their open-loop mode or with zero control gain, APMCLD treatments is identical to the MCLD treatments, whose dynamical magnetic force results from the gap variation Δx between magnets.

$$F_{\text{d}} = (\partial F_{\text{mag}}/\partial x|_{x=L_1})\Delta x = K_{\text{mag}}\,\Delta x \tag{7}$$

where $\Delta x = h_2\gamma_c + H_n(\partial w_1/\partial x|_{x=0} - \partial w_2/\partial x|_{x=L_1})$, $H_n = h_2 + h_3 + (h_1 + h_{\text{mag}})/2$, $K_{\text{mag}} = \partial F_{\text{mag}}/\partial x|_{x=L_1}$.

When the dynamical force F_{d} is generated by the controller in proportion to and derivative of the measured variation of gap between the root magnet and the coil such that

$$F_{\text{d}} = (K_{\text{mag}} + K_{\text{p}})\Delta x + K_v\,\frac{\partial \Delta x}{\partial t} \tag{8}$$

Provided that the longitudinal displacement vibration is harmonic, then

$$F_{\text{d}} = (K_{\text{mag}} + K_{\text{p}})\Delta x + K_v\,\frac{\partial \Delta x}{\partial t} = (K_{\text{mag}} + K_{\text{p}} + \mathrm{i}\omega K_v)\Delta x = K_{\text{d}}\,\Delta x \tag{9}$$

where $K_{\text{d}} = K_{\text{mag}} + K_{\text{p}} + \mathrm{i}\omega K_v$, K_{p} is the proportional control gain, K_v is the derivative control gain, ω is harmonic frequency.

Applying Hamilton's principle

$$\delta \int_{t_1}^{t_2} (T - V + W)\,\mathrm{d}t = 0 \tag{10}$$

we obtain the differential equations of motion of Section 2

$$D_t\,\frac{\partial^4 w}{\partial^4 x} - QH\left(H\,\frac{\partial^2 w}{\partial^2 x} + p\,\frac{\partial u_3}{\partial x}\right) + m\,\frac{\partial^2 w}{\partial^2 t} = 0 \tag{11}$$

$$-pE_3A_3\,\frac{\partial^2 u_3}{\partial^2 x} + Q\left(H\,\frac{\partial w}{\partial x} + pu_3 + c\right) = 0 \tag{12}$$

or, in terms of the deflection alone,

$$\left[\frac{\partial^6}{\partial x^6}-\left(\frac{QH^2}{D_t}+\frac{Qp}{E_3A_3}\right)\frac{\partial^4}{\partial x^4}+\frac{m}{D_t}\frac{\partial^4}{\partial x^2\partial t^2}-\frac{Qp}{E_3A_3D_t}\frac{\partial^2}{\partial t^2}\right]w=0 \tag{13}$$

where $Q=\frac{G_cA_c}{h_c^2}$.

In addition, Hamilton's principle yields the following beam boundary conditions:

$$x=L_2: D_t\frac{\partial^2 w}{\partial^2 x}=M_3,\quad E_3A_3\frac{\partial u_3}{\partial x}=0,\quad D_t\frac{\partial^3 w}{\partial^3 x}-QH\left(H\frac{\partial w}{\partial x}+pu_3+c\right)=S_3 \tag{14a–c}$$

$$x=L_1: -D_t\frac{\partial^2 w}{\partial^2 x}+M_2-K_{\mathrm{d}}(H-H_n)\left[(H-H_n)\frac{\partial w}{\partial x}+pu_3+c\right]=0$$

$$D_t\frac{\partial^3 w}{\partial^3 x}-QH\left(H\frac{\partial w}{\partial x}+pu_3+c\right)-S_2+\frac{1}{2}m_{\mathrm{mag}}\frac{\partial^2 w}{\partial t^2}=0$$

$$-pE_3A_3\frac{\partial u_3}{\partial x}-K_{\mathrm{d}}\left[(H-H_n)\frac{\partial w}{\partial x}+pu_3+c\right]=0 \tag{15a–c}$$

Three unknown values w, u_3, c cannot be obtained through the two Eqs. (11) and (12). Let $v=pu_3+c$, now Eqs. (11) and (12) only include two unknown values w, v. The constant c can be obtained from the supplemental condition $u_1(L_1)=0$.

To solve Eqs. (11) and (12) for harmonic vibrations, assume the solution to be of the form (Mead and Markus, 1969)

$$\begin{Bmatrix} w \\ v \end{Bmatrix}=\begin{Bmatrix} w_n \\ v_n \end{Bmatrix}\mathrm{e}^{k^*x}\mathrm{e}^{\mathrm{i}\omega^*t} \tag{16}$$

where ω^* and k^* denote the unknown complex natural frequency and characteristics values to be determined.

Substitution of Eq. (16) into (13) yields

$$k^{*6}+s_4k^{*4}+s_2k^{*2}+s_0=0 \tag{17}$$

where $s_4=-[QH^2/D_t+Qp/(E_3A_3)]$, $s_2=-m\omega^{*2}/D_t$, $s_0=m\omega^{*2}Qp/(E_3A_3D_t)$. For any ω^*, let $k_1^*,k_2^*,\ldots,k_6^*$ denote the six zeros of Eq. (17). Then, a general solution of Eq. (13) can be written as

$$w(x,t)=\sum_{j=1}^{6}C_j\mathrm{e}^{k_j^*x}\mathrm{e}^{\mathrm{i}\omega^*t} \tag{18}$$

where $C_1^*,\ldots,C_6^*$ are six constants to be determined.

Furthermore, from Eqs. (11) and (12), we have

$$v(x,t)=\sum_{j=1}^{6}g_jC_j\mathrm{e}^{k_j^*x}\mathrm{e}^{\mathrm{i}\omega^*t} \tag{19}$$

where

$$g_j=\frac{E_3A_3D_tk_j^{*5}}{Q^2Hp}-\frac{E_3A_3Hk_j^{*3}}{Qp}-\left(\frac{E_3A_3m\omega^{*2}}{Q^2Hp}+H\right)k_j^*\quad(j=1,2,\ldots,6) \tag{20}$$

With respect to ordinary beams, the differential equation of motion for Section 1 is governed by (see Fig. 2(b))

$$D_{t1}\left(\frac{\partial^4 w}{\partial x^4}\right) + m_1\left(\frac{\partial^2 w}{\partial t^2}\right) = 0 \tag{21}$$

The boundary conditions are

$$x = L, x = 0 : w(x) = w_0 e^{i\omega t}, \quad \frac{\partial w(x)}{\partial x} = 0 \tag{22a, b}$$

$$x = L_i : D_{t1}\frac{\partial^2 w}{\partial x^2} = M_i, \quad D_{t1}\frac{\partial^3 w}{\partial x^3} = S_i \tag{23a, b}$$

Assume the solution to be of the form

$$w(x,t) = \sum_{j=7}^{10} C_j e^{k_j^* x} e^{i\omega^* t} \tag{24}$$

where C_j and k_j^* denote complex values.

In a like manner, we can obtain the differential equations of motion and boundary conditions of other sections. Also, the continuous conditions of transverse displace w and rotary angle θ at $x = L_i$ ($i = 1, 2, \ldots$), yield supplementary conditions. We obtain the characteristics determinant.

$$\det[\mathrm{D}] = 0 \tag{25}$$

Eq. (25) is a non-linear, complex valued equation for unknowns ω^*, k_j^*. The problem is solved numerically using a trial and error technique in which the initial values are assumed to be those of an uncovered Euler beam. Complex double precision has been used to obtain the results. The complex frequency ω^*, the real frequency ω, and the loss factor η of the beam are related by $\omega = \sqrt{\mathrm{Re}(\omega^{*2})}$, $\eta = \mathrm{Im}(\omega^{*2})/\mathrm{Re}(\omega^{*2})$.

4. Performance of MCLD treatment

In this section, the experimental performance of the MCLD (i.e. $K_\mathrm{p} = K_v = 0$, only K_mag retained) with one or two patches as shown in Fig. 1(a) and (b) is determined and compared with the theoretical predictions as obtained from the analytical model described in Section 3. Note that in the experiments, the electro-magnetic coils in the fixed ends are replaced by permanent magnets as described in prior papers (Ruzzene et al., 2000; Baz and Poh, 2000).

4.1. Material properties and experiment

Two kinds of beam configurations with PCLD/MCLD treatments are used as test articles in this study. The first kind of clamped–clamped beams are treated with a single patch as shown in Fig. 1(a) while the second kind of beams are treated with two patches as shown in Fig. 1(b). In two-patched treatments, each patch of length of $0.1L$, $0.2L$ or $0.3L$ is placed symmetrically near each fixed end of the beam with an offset of 0.001 m. In single-patched treatments, a single patch of length of $0.2L$, $0.4L$ or $0.6L$ is also placed near the left end of the beam with an offset of 0.001 m. Moreover, a full covered beam with a small cut of 0.001 m in each end of the CL is also used as a test article, where root magnets are only placed on the left end of CL. The gap between permanent magnets is 0.001 m. The permanent magnets in the experiments are arranged in attraction and made of NdFeB blocks ($0.02\times0.005\times0.005$ m) with residual induction $B_\mathrm{r} = 1.19$ T, and magnetized through x-direction. The attractive force produced by two permanent magnets can be analyzed by Tsui's method in which the magnetic moment of a permanent magnet is represented by an equivalent

face current loop (Tsui, 1972), consequently, the magnetic stiffness K_{mag} of magnets in the experiment is 9.8E3 N/m.

The other experimental parameters are

$$h1 = 5E-4\ \mathrm{m}, \quad h2 = 3.5E3\ \mathrm{m}, \quad h3 = 2.5E-4\ \mathrm{m}, \quad b = 2E-2\ \mathrm{m}, \quad L = 0.4\ \mathrm{m},$$

$$\rho_2 = 600\ \mathrm{kg/m^3}, \quad E_1 = E_3 = 7.10E10P_a$$

$$\rho_1 = \rho_3 = 2.7E3\ \mathrm{kg/m^{3^3}}, \quad \lg G = 0.1015 \lg \frac{\omega}{2\pi} + 5.1817$$

$$\eta = 3.3 \times 10^{-6} \times \left(\frac{\omega}{2\pi}\right)^3 - 4.33 \times 10^{-4} \times \left(\frac{\omega}{2\pi}\right)^2 + 2.09 \times 10^{-2} \times \left(\frac{\omega}{2\pi}\right) + 0.1722$$

Each end of the beam is subject to the sinusoidally varying transverse displacement $W_0 e^{i\omega^* t}$. Note that only symmetrical modes of beams with two patches are excited. The response of beam at $x = 0.5L$ is measured. First several natural frequencies (f_r) and modal loss factors (η_r) are then extracted using the half-power bandwidth method (Ahid et al., 1985). Tables 1–3 list frequencies and loss factors for the first and third modes of beams treated with different MCLD treatments. The predictions are in good agreement with the experimental results.

4.2. Optimal placement strategies of discrete patches

Fig. 3(a)–(c) illustrates the variation of loss factors of beams for the first three modes with damping length. The results indicate that, at the first mode, using full covered MCLD treatment it has almost no

Table 1
Effect of PCLD/MCLD with two patches (L_0: total length of two patch)

L_0/L		Calculation				Experiment			
		f_1 (Hz)	η_1	f_3 (Hz)	η_3	f_1 (Hz)	η_1	f_3 (Hz)	η_3
0.2	PCLD	17.35	0.0195	89.15	0.0233	17.40	0.0198	89.38	0.0247
	MCLD	16.90	0.0321	87.30	0.0303	16.88	0.0318	87.43	0.0310
0.4	PCLD	18.23	0.0612	74.46	0.0435	18.34	0.0610	74.60	0.0446
	MCLD	16.97	0.0900	76.03	0.0437	16.89	0.0890	75.96	0.0441
0.6	PCLD	16.35	0.0772	85.94	0.1138	16.45	0.0762	85.67	0.1144
	MCLD	14.80	0.1080	85.94	0.1137	14.34	0.1025	85.90	0.1148

Table 2
Effect of PCLD/MCLD with a sing patch (L_0: length of a sing patch)

L_0/L		Calculation				Experiment			
		f_1 (Hz)	η_1	f_3 (Hz)	η_3	f_1 (Hz)	η_1	f_3 (Hz)	η_3
0.2	PCLD	17.48	0.0417	80.09	0.0267	17.08	0.0396	80.79	0.0289
	MCLD	16.83	0.0509	79.72	0.0273	16.43	0.0518	80.43	0.0286
0.4	PCLD	14.67	0.0505	91.80	0.2961	14.62	0.0517	90.95	0.2892
	MCLD	13.96	0.0572	91.95	0.2989	13.33	0.0570	91.03	0.2980
0.6	PCLD	16.32	0.0752	86.27	0.1229	16.90	0.0746	85.87	0.1287
	MCLD	14.83	0.0992	86.10	0.1227	14.54	0.0946	85.65	0.1213

Table 3
Effect of full covered PCLD/MCLD

	Calculation				Experiment			
	f_1 (Hz)	η_1	f_3 (Hz)	η_3	f_1 (Hz)	η_1	f_3 (Hz)	η_3
PCLD	21.84	0.3213	82.10	0.4450	21.71	0.3245	81.79	0.4346
MCLD	21.83	0.3214	82.10	0.4451	21.68	0.3252	81.56	0.4334

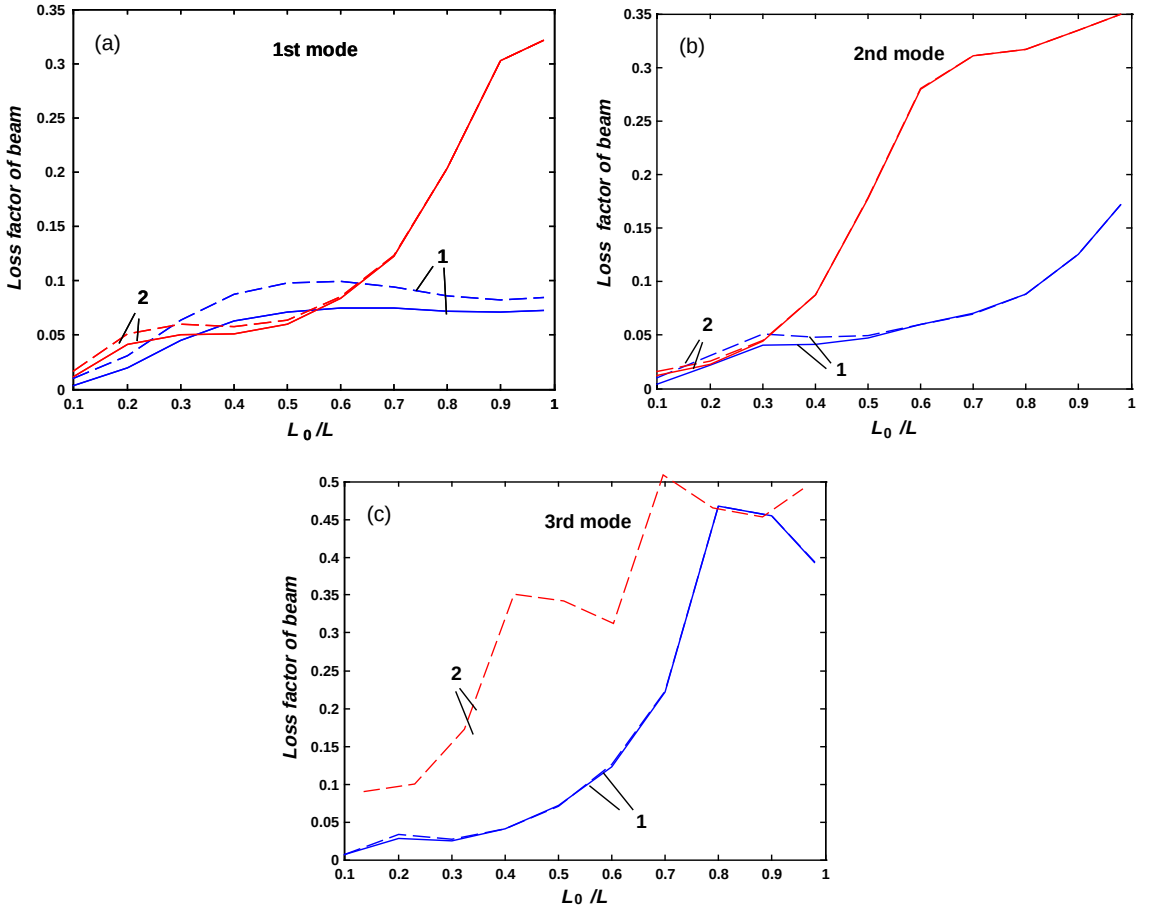

Fig. 3. Variation of loss factors of beams with damping length (1: two patches; 2: a single patch; -: PCLD; - - -: MCLD). (a) First mode; (b) second mode; (c) third mode.

effects on loss factor. In this point, it differs from that of the cantilever beam with full covered MCLD treatments, in which MCLD treatments induce significant damping improvement (Ruzzene et al., 2000; Baz and Poh, 2000). However, using single-patched MCLD treatments it can enhance the damping of beams when damping layer is short whereas two-patched MCLD treatments can significant enhance damping even though the total length L_0 of the two patches is close to the full length of beam. Such phenomena are also observed in Tables 1–3. The results indicate also that the damping improvement resulting from two-patched MCLD treatments is more apparent for the first mode compared to the corresponding performance of

single-patched treatments when the length of damping layer is between $0.3L$ and $0.65L$ under considered magnetic force. It is found that, however, for the second and third modes, in both of the MCLD segmented treatments, long damping layer induces less improvement of damping characteristics whereas short damping layer can simultaneously enhance damping.

It is evident that arranging the magnets at a smaller gap (consequently higher magnetic stiffness) is more effective in enhancing damping characteristics. Fig. 4(a)–(c) illustrates the effect of magnetic stiffness K_d on loss factors for the first three modes using both the MCLD segmented treatments. Note that for the MCLD, K_d is identical to K_{mag}. The results in Fig. 4 are obtained with such parameters as follows. In two-patched treatment, each segment is $0.25L$ long. In single-patched treatment, the segment is $0.5L$ long. The other parameters are identical to those in the experiment. Curves 1 illustrate that, in two-patched MCLD treatments, increasing the magnetic stiffness increases rapidly the loss factor for the first mode in a nolinear way whereas significant improvements of damping for the second and third modes are obtainable only when the magnetic stiffness is very high. Curves 2 illustrate that, in single-patched MCLD treatments, increasing the magnetic stiffness induces less damping improvement for the first two modes and also significant improvement of damping for the third mode is obtainable only when the magnetic stiffness is very

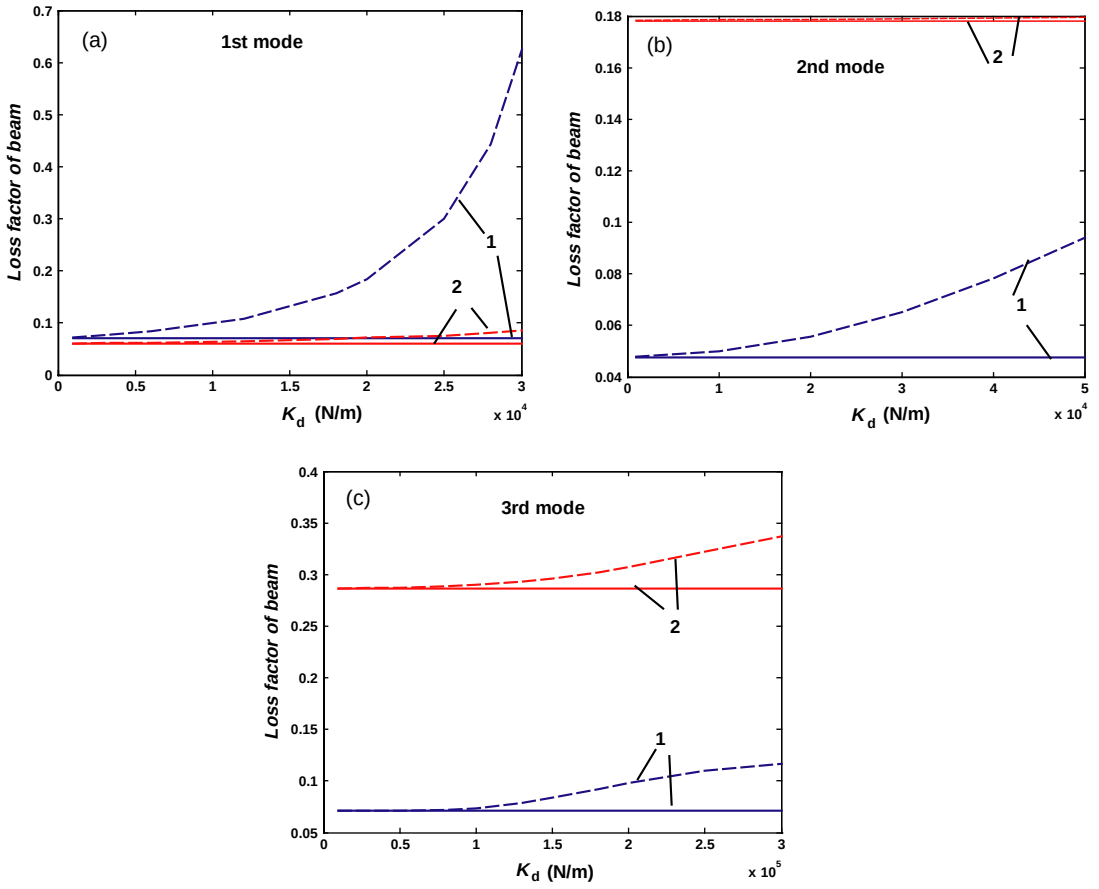

Fig. 4. Variation of loss factors of beams with K_d (1: two patches; 2: a single patch; -: PCLD; - - -: MCLD) (a) first mode; (b) second mode; (c) third mode.

high. The results indicate also that one or two patches MCLD treatment has its own advantage compared with each other. Such results help us select the optimal configurations of discrete patches of MCLD treatments in different operation conditions.

5. APMCLD treatments using several control strategies

Usually, the first mode plays an important role in structural vibration, hence in these cases, two-patched MCLD treatments may be considered as feasible approaches to suppress structural vibrations. However, obtaining higher magnetic stiffness for controlling higher modes is rather difficult and the ability of MCLD to compensate for changes in the operating or environmental conditions is limited. In order to control structural vibrations over a broad band frequency, the APMCLD treatment as described in Section 2 is a natural extension to the MCLD treatment. In this section, the emphasis is placed on investigating theoretically damping performances of the two-patched APMCLD treatment as shown in Fig. 1(b) with VEM shear modulus G under different control strategies. Such investigation will help to develop design guidelines.

Several control strategies are considered to activate the magnetic actuators as follows: (1) simple proportional control; (2) simple derivative control; (3) combined proportional and derivative control. The analytical parameters chosen are: each patch is $0.25L$ long (i.e. $L_0/L = 0.5$), $\beta = 0.4$, the other parameters are identical to those in the experiment unless stated.

Fig. 5(a)–(c) illustrates the variation of loss factor η of the beam with VEM shear modulus G for the first three modes. Curves 1 are obtained with PCLD treatment. Curve 1 in Fig. 5(a) illustrates that, in the PCLD treatment, a maximal loss factor is only obtainable at a particular value of G_{opt} and that as G deviates from G_{opt}, loss factors for the first mode would decrease rapidly. The same phenomenon was also observed for the fully covered damped sandwich beam (Ahid et al., 1985). In practice, G would decrease because of temperature rise in operation, and the VEM of optimal shear modulus G is not always available. Therefore the better damping is not easily realized.

Curves 2 are obtained with MCLD treatment ($K_{\text{mag}} = 9.8\text{E}3$ N/m). Curve 2 in Fig. 5(a) indicates that the improvement of MCLD for $G < G_{\text{opt}}$ is significant whereas the improvement for $G > G_{\text{opt}}$ become little. The phenomenon may be explained as follows. Increasing G increases the dynamical forces acting on the CL. Consequently, the ratio of dynamical magnetic force F_{d} to the maximal dynamical force $F_{\max}$ acting on the CL is reduced not enough to affect deformation of sandwich beam. Such results reveal that significant improvement of damping characteristics for the first mode exists over a broad G range. This implies that the limitation to VEM of MCLD treatments is less than that of PCLD treatments and the degeneration of damping characteristics because of temperature rise can be compensated for to some extent using the MCLD.

Curves 3 are obtained with proportional controller that has proportional gain $K_{\text{p}} = 8.4\text{E}3$ along with MCLD treatment ($K_{\text{mag}} = 9.8\text{E}3$ N/m). Note that the MCLD treatment at different gaps between permanent magnets is identical to APMCLD treatments using a proportional controller for different gains. Since the shear strain of the second and third modes is too small to produce strong dynamical magnetic force (Kung and Singh, 1998), the ability to control higher modes vibration is still limited over a broad range of G as shown from curves 2 ($K_{\text{p}} = 9.8\text{E}3$) and curve 3 ($K_{\text{p}} = 1.82\text{E}4$) in Fig. 5(b) and (c). Although higher modes can be suppressed by increasing proportional gain K_{p} as shown in Fig. 4(b) and (c), high gain would cause active control system unstable and is difficult to implement.

Curves 4 and 5 are obtained with derivative controller that has derivative gain $K_v = +100$ and $K_v = -100$ respectively along with MCLD treatment ($K_{\text{mag}} = 9.8\text{E}3$ N/m). It can be seen that significant improvements can be obtained for higher modes with negative derivative feedback controller whereas less improvement of damping can be obtained with positive derivative feedback controller but for the second

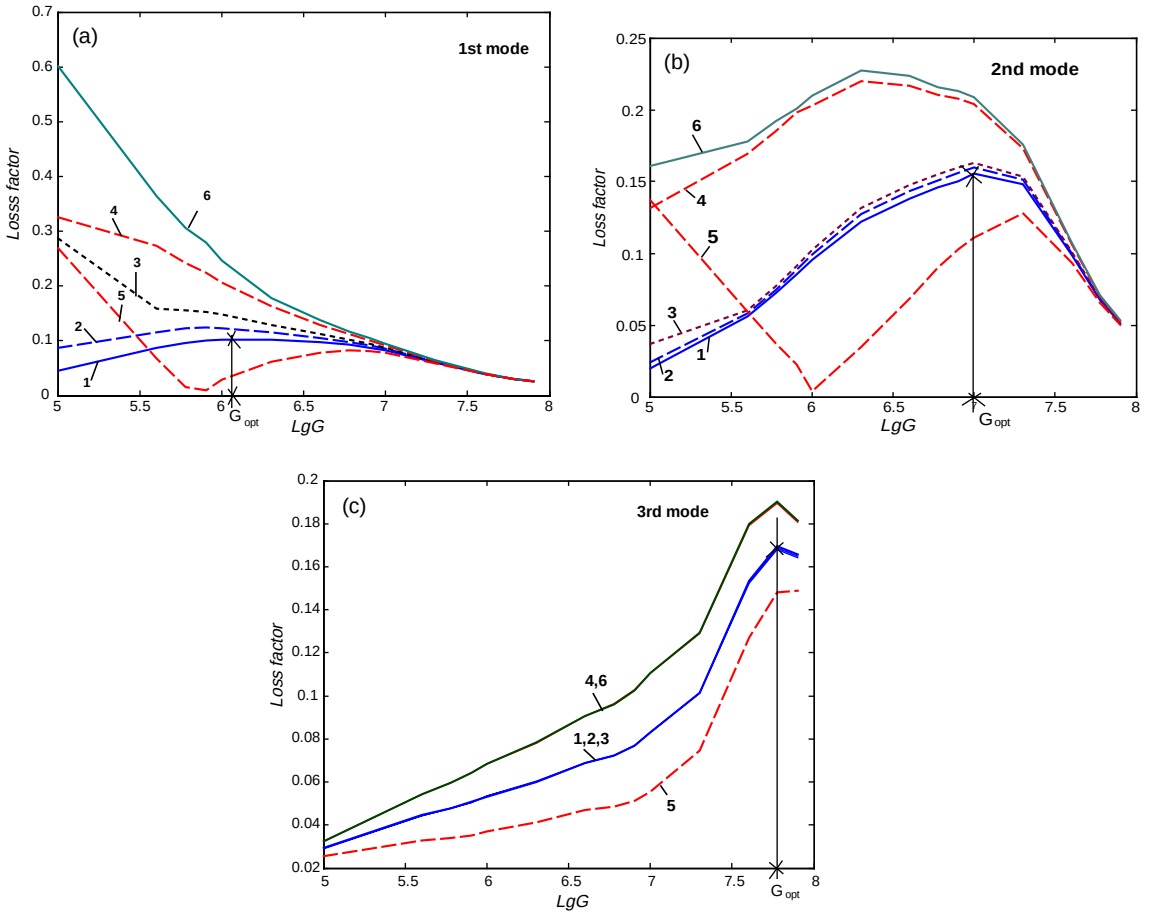

Fig. 5. Variation of loss factor η with VEM shear modulus G. (a) First mode, (b) second mode, (c) third mode 1: PCLD; 2: MCLD ($K_{\text{mag}} = 9.8\text{E}3$ N/m); 3: proportional ($K_{\text{mag}} = 9.8\text{E}3$ N/m, $K_{\text{p}} = 8.4\text{E}3$); 4: derivative ($K_{\text{mag}} = 9.8\text{E}3$ N/m, $K_v = -100$); 5: derivative ($K_{\text{mag}} = 9.8\text{E}3$ N/m, $K_v = 100$); 6: combination ($K_{\text{mag}} = 9.8\text{E}3$ N/m, $K_{\text{p}} = 8.4\text{E}3$, $K_v = -100$).

mode under lower VEM shear modulus. This may be explained as follows. When the APMCLD beam with derivative controller vibrates, at the moment variation of gap between magnets becomes zero, actuator with negative derivative controllers produces a magnetic repulsive force resulting in a shear strain distribution $\gamma_0(x)$ in damping layer which is in counter-phase with the shear strain distribution $\gamma_c(x)$ at the moment the gap becomes minimal resulting from the deflection deformation of the sandwich section. Thus the variation of VEM shear strain per cycle of vibration increases and consequently enhance energy dissipation. Similarly, at the moment variation of gap between magnets becomes zero, actuator with positive derivative controller produces magnetic attractive forces resulting in shear strain $\gamma_0(x)$ in damping layer which is in phase with the shear strain distribution $\gamma_c(x)$ at the moment the gap becomes minimal resulting from the deflection deformation of the sandwich section. Not that since the $\gamma_0(x)$ is much larger than $\gamma_c(x)$ for the second mode with low VEM shear modulus, the variation of VEM shear strains per cycle of vibration exceeds strain of PCLD treatment and significant improvements can also be obtained in this case as shown in Fig. 5(b) whereas in other cases, the variations of VEM shear strains per cycle become smaller than strains of PCLD treatment and consequently decreases loss factors of beam.

Curves 6 are obtained with combined proportional and derivative controller that has proportional gain $K_p = 8.4E3$ and derivative gain $K_v = -100$ along with MCLD treatment ($K_{mag} = 9.8E3$ N/m). Since the proportional controller plays an important role in suppressing the first mode of vibration while the derivative controller plays a dominated role in controlling the second and three modes of vibration, higher damping can be obtained for the first three modes simultaneously.

Note that the MCLD treatment still plays an important role in controlling vibration for low order modes even though active control system falls in failure.

6. Conclusions

This paper has presented a new class of active and passive magnetic constrained layer damping treatments. The predictions of model are validated experimentally using three-layer clamped–clamped beams which are treated with fully or segment MCLD treatments. Such conclusions are drawn.

(1) Full treatments with MCLD induce less improvement of damping characteristics. The improvement of damping characteristics using two-patched MCLD treatment becomes more apparent for the first mode compared to the corresponding performance using single-patched MCLD treatment when the total length of damping layer is between $0.3L$ and $0.65L$ under considered magnetic force. It is found that, however, for higher modes, in both the two kinds of segmented MCLD treatments, long damping layer induces less improvement of damping characteristics while short damping layer can enhance damping for broad band structural vibration.

(2) The interaction between magnets and damping layers is sensitive to the damping layer's shear modulus G. The improvement of damping characteristics exists over a broad G range for $G < G_{opt}$.

(3) The APMCLD treatment could present a viable means for controlling high amplitudes of vibration over a broad band frequency. It has less improvement of damping characteristics for higher modes using simple displacement positive feedback controller whereas the higher modes can been suppressed effectively using velocity negative feedback. The combination of displacement and velocity feedback can suppress the first several modes simultaneously. Moreover, the MCLD treatment still plays an important role in damping structural vibrations even though the active control falls in failure.

References

Ahid, D., Nashif, David, I., 1985. Vibration Damping. Wiley, New York.

Baz, A., Poh, S., 2000. Performance characteristics of the magnetic constrained layer damping. Shock and Vibration 72, 81–90.

Changhwan, C., Kyihwan, P., 1999. Self-sensing magnetic levitation using a LC resonant circuit. Sensor and Actuators A 72, 169–177.

Kung, S., Singh, R., 1998. Vibration analysis of beams with multiple constrained layer damping patches. Journal of Sound and Vibration 212 (5), 781–805.

Lin, C., 1998. Active suppression of the vibration of a flexible beam using eddy current sensor. Journal of Sound and Vibration 217 (2), 387–395.

Mead, D.J., Markus, S., 1969. The forced vibration of a three-layer damped sandwich beam with arbitrary boundary condition. Journal of Sound and Vibration 10 (2), 163–175.

Reader, W., Sauter, D., 1993. Piezoelectric composite with active constrained layer treatments. Proceeding of DAMPING'93 GBB 1–18.

Ruzzene, M., Oh, J., Baz, A., 2000. Finite element modeling of magnetic constrained layer damping. Journal of Sound and Vibration 236 (4), 657–682.

Shields, W. et al., 1998. Control of sound radiation from a plate into an acoustic cavity using active piezoelectric damping composites. Journal of Smart Material Structures 7, 1–11.

Tsui, B., 1972. The effect of intrinsic magnetic properties on permanent magnetic repulsion. IEEE. Trans. Magnetics MAG-8, 2.